Proceedings of the Combustion Institute, Volume 29, 2002/pp. 361–368

INHIBITION OF PREMIXED METHANE/AIR FLAMES BY WATER MIST

S. PAUL FUSS,[1,*] EZRA F. CHEN,[1] WENHUA YANG,[2] ROBERT J. KEE,[2] BRADLEY A. WILLIAMS[1]
AND JAMES W. FLEMING[1]

[1]*Combustion Dynamics Section, Code 6185*
Chemistry Division
Naval Research Laboratory
Washington, DC 20375-5342, USA
[2]*Engineering Division*
Colorado School of Mines
Golden, CO 80401, USA

The effect of submicron water drops on the burning velocity of methane/air mixtures was investigated. Results are compared to the suppression effect of water vapor, gaseous thermal agents N_2 and CF_4, and chemical agent CF_3Br to determine if the theoretical thermal suppression effect expected for water mist can be experimentally achieved. These studies lay the groundwork (both experimental and modeling) for the effects of larger drops as well as for drops with solutes. Stoichiometric mixtures were stabilized at atmospheric pressure on one of two nozzle-type burners, producing cone-shaped flames. Burning velocities were determined using the total area method. An atomizer was used to produce water mist with a mean drop diameter of less than 1 μm, which was delivered as part of the reactant stream. Studies were carried out using both dry and humidified air. On a mass basis, the burning velocity of N_2- and CF_4-inhibited flames exhibited similar characteristics. Water vapor was observed to be more effective than N_2 or CF_4, but less effective than the same mass of water mist, consistent with thermodynamic analyses. Water mist inhibition results were well predicted by a recently developed multiphase flame model. Under these conditions, the burning velocity reduction effectiveness of water mist is approximately 3.5 times greater on a mass basis than for N_2 and CF_4 and is comparable to modeled data for CF_3Br-inhibited flames.

Introduction

The ban on production of halons has prompted renewed interest in the use of water as a fire-suppression agent. Since water is ubiquitous, non-toxic, environmentally benign, and has a high heat capacity per unit mass, it is in many respects an ideal fire-suppression agent. Water is a liquid under normal temperature rather than a gas like Halon 1301 (CF_3Br) and current fluorocarbon alternatives. Many engineering issues arise concerning drop size distribution, delivery into and throughout the space to be protected, and complexity of the generation system. Current fire-suppression systems based on water use far more agent than should be required based on a comparison of water's sensible enthalpy with that of nitrogen or carbon dioxide. In attempting to broaden the range of fire protection applications for which water can be used, it is desirable to determine the degree to which the effect predicted based on water's thermal properties can actually be achieved under favorable conditions.

Furthermore, water may be useful as a delivery method for non-volatile chemical fire suppressants. A number of elements and compounds have been demonstrated to exhibit far better chemical fire suppression than the bromine in CF_3Br [1]. Most of these contain metallic elements and have very low volatility. Water is a good solvent for many metallic compounds; thus, it may be useful as a dispersing agent for many new suppressants. Since water's effect on flames is almost entirely thermal [2], it is unlikely to interfere with the chemical activity of a solute.

The laminar burning velocity is a fundamental property of a flammable gas mixture, and as such the reduction in laminar burning velocity is frequently used as an indicator of the effectiveness of an inhibiting agent [3–7]. There are a variety of methods to measure laminar burning velocity [8]. We employed the total area method, a widely used technique due to its relative simplicity. Experimental efforts focused on characterizing the inhibition effectiveness of water mist by measuring the reduction in burning velocity of methane/air flames inhibited by water

---

[*] American Society for Engineering Education NRL Postdoctoral Fellow (1999–2000). Current address: Bureau of Alcohol, Tobacco, and Firearms, Fire Research Laboratory, Rockville, MD 20850, USA.

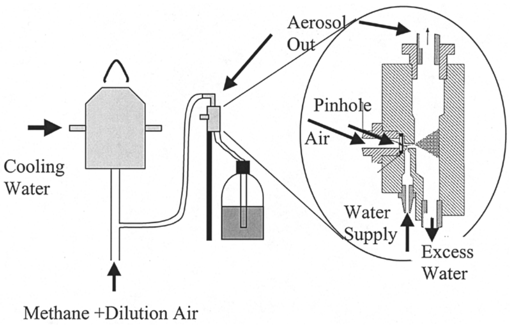

FIG. 1. Schematic of experimental configuration. Enlarged image is from TSI Instruction manual, part number 133076—Rev. F.

mist. Additional measurements were made with water vapor, N_2, and CF_4 as inhibiting agents. These measurements served as benchmarks to validate the experimental technique through comparison with data from previous studies.

Thermodynamic analyses and modeling efforts were also carried out to provide insight into the suppression mechanisms and aid in interpreting the data. Theoretical analyses, based on large-activation-energy asymptotic approximations, have been successful in describing how the burning velocity of a premixed flame is affected by water-drop size and loading [9,10]. Subsequently, computational models were developed, which extended the submodels of two-phase heat and mass transfer, incorporated elementary combustion chemistry (GRI-MECH 3.0 [11]), and included multicomponent molecular transport [12]. The two-phase premixed-flame model [12] is based on an Eulerian-Lagrangian algorithm that is analogous to that reported by Lentati and Chelliah in their analysis of non-premixed counterflow flames [13]. The present experimental and modeling studies quantify the thermal, physical, and chemical effects of water mist as a fire-suppression agent.

Experimental Procedure

Studies were carried out on two burners to establish premixed methane/air flames at atmospheric pressure. The two burners had different diameters in order to extend the water loading due to airflow requirements in the mist generator as discussed below. For similar flame conditions, relative burning velocity results on either burner were the same within the experimental uncertainty. Burner 1 was a tubular burner (Hencken Research Technologies, Livermore, California) enclosed in a Plexiglas housing. The burner nozzle exit diameter was 5.4 mm, and the burner was cooled with water at 22 °C. The burner had provisions for a coflow; however, none was used for these measurements. Burner 2 was a Naval Research Laboratory–designed converging nozzle with an exit diameter of 1.0 cm. This burner was cooled with a low flow (~0.02 lpm) of water. The burner was enclosed in a Plexiglas enclosure. Stoichiometric methane/air flames were stabilized on each burner for a range of total gas flows (burner 1: 0.8–1.75 standard liters/minute [SLPM]; burner 2: 2.5–4.1 SLPM) determined using mass flow control devices (Sierra Model 860C). Laboratory supply air was filtered and dried (Whatman model 64-01) to remove oil, water, and particulates larger than 0.1 μm in diameter. The relative humidity of the filtered airstream was measured to be less than 5%. Ultra-high purity methane (99.99%; Scott Specialty Gases) was used as the fuel gas. For the humidified air studies, both airstreams (aerosol-generating air and dilution air) were humidified using separate 6-cm diameter bubbler humidifiers containing a bed of 6-mm diameter glass beads achieving a relative humidity greater than 90%. The airstream water vapor content was measured using a hygrometer (Vaisala model HMI41-HMP46). Both dry and humid airstreams were studied in order to examine the effects of mist evaporation away from the flame.

Burning velocities were measured using the total area method as described by Andrews and Bradley [8]. The luminous flame surface was imaged with a digital camera in a 640 × 480 pixel array. Images were captured and averaged over a period of approximately 4s (20 samples) using custom-designed applications (LabView, National Instruments). An eighth-order even polynomial was fit to each image and integrated to give the flame surface area. Integration was performed from the flame cone axis to a radius of typically 0.35 cm (burner 1) and 0.56 cm (burner 2); these diameters were larger than the radius of the burner at the exit plane (0.27 and 0.50 cm, respectively). The larger radii were chosen to match the furthest extent of the visible flame zone. The measured flame area and thus the derived absolute burning velocity depended on the radius used in the data analysis. All burning velocity measurements were normalized by an uninhibited burning velocity measured under the same conditions and derived in the same manner. The maximum difference in the normalized burning velocity was less than 10% for a fit radius range of 0.35–0.27 cm for burner 1 and 0.56–0.5 cm for burner 2 over the entire range of flow rates investigated. Thus, the use of a normalized value removes the requirement for an absolute value.

A schematic of the experimental configuration is shown in Fig 1. For the inhibited flame measurements, agents were delivered to the flame with the reactant mixture. For the water-mist studies, one airstream was passed through an atomizer (TSI model 3076) that generated submicron-sized water drops, which were entrained in the premixed flow. Water

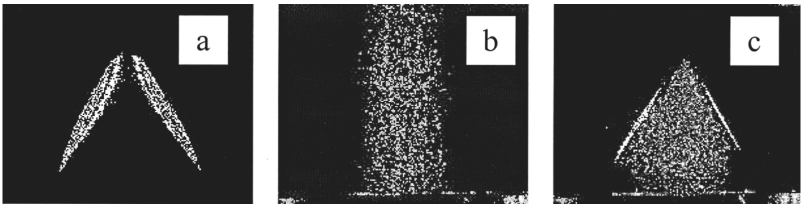

FIG. 2. (a) Image of premixed methane/air flame stabilized on burner 2. (b) Image of water mist (no flame) as it exits burner 2 illuminated with a ~1-mm thick light sheet (doubled Nd:YAG laser) centered in the middle of the burner exit and parallel to the camera. Scatter from the burner exit can be seen in the bottom of the image. (c) Image of laser-illuminated water mist and methane/air flame showing disappearance of the mist at the flame boundary.

concentrations were adjusted by mixing with dilution air. The pressurized aerosol generating airstream flowed through a small orifice (343 or 150 μm depending on mass loading of water desired), producing a high-velocity jet. Water was drawn from a reservoir through a small tube as a result of the pressure drop and broken into drops by the airstream/water jet impacting the opposing surface. Drops small enough to be entrained in the airstream were carried out of the atomizer. Larger drops and residual liquid were returned to the reservoir. The amount of water exiting the atomizer was calibrated by measuring the change in mass of the water in the reservoir with time for a fixed airflow rate. In order to make a more accurate measurement of the change in water mass, a small test tube containing water was inserted inside the empty reservoir during calibration runs.

Our multiphase, premixed modeling results show that in general, for a given mass loading, smaller drops are more effective in reducing burning velocity than larger drops. However, one interesting aspect of the models is the observation of a small-drop limiting behavior. In the small-drop limit, the burning velocity depends on the water mass loading, but not the drop diameter. Drops with diameters at or below the limit fully evaporate just upstream of the flame or within the flame zone itself. Drops above this size limit can penetrate through the flame, completing their evaporation in the postflame gases. Only that portion of the drop mass that evaporates in the immediate flame zone is effective in affecting the burning velocity. Thus, to use water drops most efficiently to reduce burning velocity, the drops should be at or below the limit size. However, there is no suppression benefit on a mass-weighted basis to reducing drop size further.

Based on the computational model for stoichiometric methane/air flames, the limiting drop diameter is about 10 μm. Since complete evaporation of the mist is possible for drops below the limit size, the inhibited burning velocity is predicted to depend on the water mass loading and to be independent of mist drop size.

The atomizer specifications state a mean drop diameter of 0.35 μm for the recommended airflow rate of 3.0 SLPM using the 343-μm orifice. This value is well below the limiting drop diameter predicted by the model. This flow rate, however, was too high to stabilize a stoichiometric flame on burner 1 and left little room for variation on burner 2. Experiments showed that reducing the airflow rate to a range where a stoichiometric flame could be stabilized resulted in a significant reduction in the performance of the atomizer. Replacing the 343-μm orifice in the atomizer with a 150-μm orifice alleviated this issue. The smaller orifice produced a satisfactory mist at airflow rates as low as 0.65 SLPM. These conditions extended the range of achievable water-mist concentrations. Drop size investigations using a phase Doppler particle analyzer (Dantec Measurement Technology) indicated that there was no measurable change in the upper size limit for the change in flow rate or orifice size; all of the drops were less than 1.5 μm in diameter. Burning velocity results using both atomizer configurations were in good agreement and are presented together here, as well data for both burners. While the change in configuration of the atomizer may have changed the submicron drop size distribution, both configurations produced drops that were still well below the predicted limiting drop diameter and thus small enough to be completely consumed by the flame. Evidence of the complete evaporation of the drops in the flame was obtained by imaging the flame and drops (illuminated with a frequency-doubled Nd:YAG laser light sheet). Fig. 2 depicts images of (1) a premixed methane/air flame only, (2) mist generated with the 343-μm atomizer orifice, and (3) mist and flame. As can be seen in the figure, there is an abrupt disappearance of the mist scattering just before the visible flame surface. Similar results were observed for the 150-μm orifice.

Water mist in the reactant stream was monitored by 90° scattering of a helium-neon laser (0.6328 μm) detected with a photomultiplier tube (PMT). The laser beam was chopped mechanically at 1000 Hz, and a reference beam was split off before passing over the burner. The reference beam intensity was monitored by a photodiode. The PMT and reference signals were processed with a lock-in amplifier

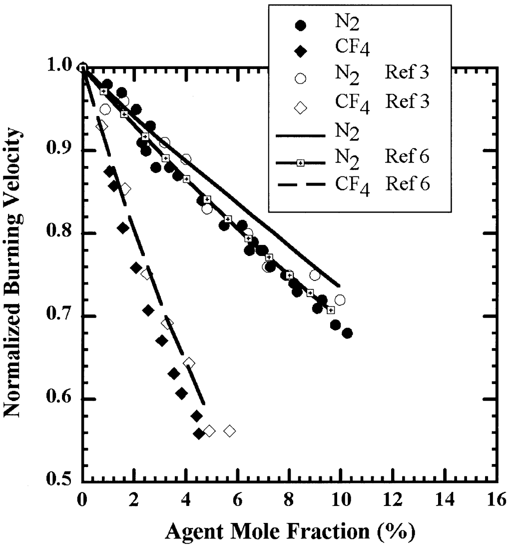

FIG. 3. Premixed methane/air burning velocity as a function of agent mole fraction, normalized by the uninhibited burning velocity: present study (closed symbols), data from Ref. [3] (open symbols), calculations from the present study using PREMIX [15] and GRI-MECH 3.0 [11] (solid line), and calculations from Ref. [6] (dashed line and line with square/cross).

(EG&G Instruments, model 7265 DSP) and integrated over a period of 0.5 s. The laser beam was positioned just above the nozzle exit. In order to monitor the water mist and obtain a simultaneous flame surface area measurement, the flame image was recorded through a filter (Corning CS7-59) to remove the He-Ne scattering. Scattering intensity measurements with and without a flame present were identical, indicating no evaporation due to the presence of the flame at the point of measurement. The scattering intensity was calibrated to a mist delivery rate by correlating the scattering signal recorded with the amount of water that was removed from the mist reservoir in a fixed period of time.

The normalized mist scattering intensity showed a linear correlation with dilution by humidified air with a slope of 0.96 ± 0.04. Dilution is defined as the ratio of the volumetric flow of the original mist-laden stream to the total stream volumetric flow (mist and diluting air). The linear correlation suggests that there was minimal evaporation due to dilution with the humidified air. The mist scattering intensity reduction by dilution with dry air decreased with a nonlinear dependence on dilution, consistent with partial evaporation of the mist. Comparison of the wet and dry air dilution results and the gas flow rates required for the dry air flame studies indicates that at the highest dilution (lowest mist concentrations), up to 35% of the mist could have evaporated prior to exiting the burner. It has been shown [14] that the effectiveness of thermal inhibition agents, of which water is one, is independent of the location of heat absorption relative to the flame. However, thermocouple measurements of the gas stream at the burner exit indicated that the reduction in the temperature of the mist-laden airstream following dilution by dry air was less than 1 °C due to heat exchange with the tubing and burner. Since the heat of vaporization for water accounts for approximately 45% of its sensible enthalpy over a temperature range from 300 to 1600 K, any water that evaporates prior to leaving the burner is expected to be less effective.

Results and Discussion

In order to establish the validity of the experimental protocol, burning velocities were measured for methane/air flames inhibited by N_2 and CF_4. Since these are both gases at room temperature, delivery into the flame is straightforward, and there is minimal uncertainty in determining concentrations compared with water. Experimental results are presented in Fig. 3. The open symbols are taken from an experimental study [3] that utilized a procedure similar to the one described here. The experimental results are in good agreement with those published. Also shown in Fig. 3 are PREMIX calculations from Ref. [6] and calculations for N_2-inhibited flames carried out in the present study using PREMIX [15] and GRI-MECH 3.0 [11]. Results for the gas-phase studies are also in good agreement with these modeling predictions. Results show that on a molar basis, CF_4 is ~3 times more effective than N_2 at reducing the burning velocity of methane/air flames.

Normalized burning velocities for methane/air flames are plotted in Fig. 4 on a mass basis for dry flames inhibited with N_2, CF_4, water vapor, water mist, and CF_3Br. When compared on a mass basis, N_2 and CF_4 show comparable effectiveness. The measured water-mist effectiveness compares favorably with the CF_3Br modeled data from Refs. [6] and [16].

Also shown in Fig. 4 are results for wet flames (containing 1.5% water vapor by mass in the premixed gases) inhibited by water mist (gray circles). The mist effect on the normalized burning velocity of the wet or dry flames are comparable (similar slopes within experimental uncertainty), suggesting that the mist exhibits similar thermal effects in both flames. This indicates that any dilution-caused evaporation prior to introduction of the mist into the dry flame did not have a significant effect. The mist may be slightly more effective in the humidified flame (which would be consistent with some evaporation in the dry flame measurements), but any difference is less than the scatter in the data. A similar mist

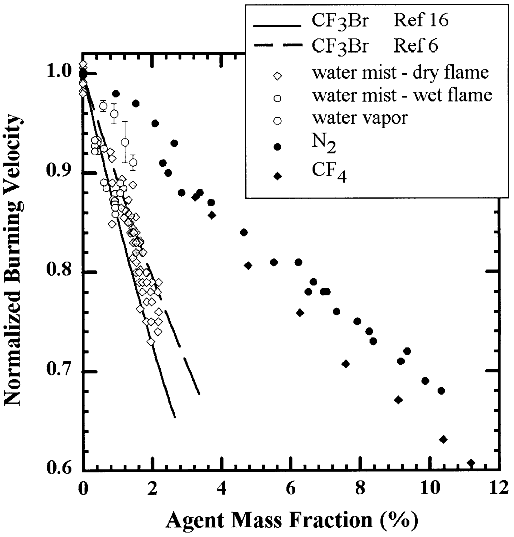

FIG. 4. Premixed methane/air burning velocity as a function of agent mass fraction, normalized by the uninhibited burning velocity inhibited by 0.35-μm water mist in dry flame (gray diamond), 0.35-μm water mist in "wet" flame containing 1.5% mass fraction water vapor in the premixed gases (gray circle), water vapor (open circle), N_2 (black circle), CF_4 (black diamond), and CF_3Br (dashed line from Ref. [6]; solid line from Ref. [16]).

effectiveness in each flame would be expected if no prior mist evaporation occurred. To verify this, we measured the effect of nitrogen addition to both flames. The same slope ($\pm 3\%$) in the normalized burning velocity reduction was observed for each flame.

The results in Fig. 4 are reasonable based on the thermodynamic properties of the various agents as presented in Table 1. Column 2 lists the sensible enthalpy per unit mass required to raise the temperature of each agent from 300 to 1600 K [17]. On a mass basis, N_2 and CF_4 have comparable values. The value for water mist, which includes the heat of vaporization at 1 atm, is roughly twice that of water vapor and 3.5 times higher than that for N_2, CF_4, or CO_2. CO_2, not listed in Table 1, has a sensible enthalpy ($H_f^{1600K} - H_f^{300K} = 1.5$ kJ/g) [17] that is close to that for N_2 and CF_4. Additionally, the extinction mass fraction for heptane cup burner flames is similar for N_2, CF_4, and CO_2 [18]. Since these agents exhibit predominantly thermal inhibition characteristics, one would expect a similar relationship to exist between the concentrations required to bring about a reduction in the burning velocity.

To evaluate the observed inhibition effectiveness of water mist with the other agents, linear least squares fits were applied to the burning velocity measurements. These fits were used to compare the inhibitor concentration required to reduce the laminar burning velocity by 20% from the uninhibited case. The results are given in Table 1, column 4, on a mass basis and Table 1, column 5, on a molar basis. Column 4 shows that, on a mass basis, the measured concentration of water mist needed to reduce the burning velocity by 20% was 30%–35% of the concentrations required for N_2 and CF_4, in good agreement with the thermodynamic estimate.

Column 4 of Table 1 also shows that the mass fraction of water mist required for a 20% reduction in burning velocity is comparable to the estimated value for CF_3Br. Previous studies [19,20] have shown that, in non-premixed flames, CF_3Br is 2–2.5

TABLE 1

Comparison of thermal properties and suppression efficiencies for N_2, CF_4, water vapor, water mist, and CF_3Br

	$(H_f^{1600K} - H_f^{300K})^a$				$(H_f^{1600K} - H_f^{300K})*(X_{agent}/X_{O2})$
Agent	(kJ/g)	(kJ/mol)	Mass Fraction	Mole Fraction	(kJ/mol)
N_2	1.5	42	6.3 ± 0.4	6.2 ± 0.4	14.6 ± 0.9
CF_4	1.4	122	5.5 ± 0.4	1.9 ± 0.2	12.1 ± 1.3
H_2O (vapor)	2.9	53	3.3 ± 0.2	5.0 ± 0.3	14.3 ± 0.8
H_2O (mist)	5.2	93	1.7 ± 0.1	2.6 ± 0.2	13.2 ± 1.1
CF_3Br	0.85	126	1.9^b	0.4^b	2.5

Note: Columns 2 and 3 list the sensible enthalpy of each agent for a temperature range of 300–1600 K. The value for water mist includes the heat of vaporization at 1 atm. Columns 4 and 5 contain the experimental mass and mole fractions of the total flow, respectively, for the conditions required to reduce the burning velocity by 20% from the uninhibited case. Column 6 is the product of column 3 with the ratio of agent mole fraction (X) to O_2 mole fraction for the condition where the burning velocity is reduced by 20% from the uninhibited case. Uncertainties are derived from the standard deviations in the fits to the data.

[a] Calculated from data in Ref. [17].

[b] Data from Ref. [6].

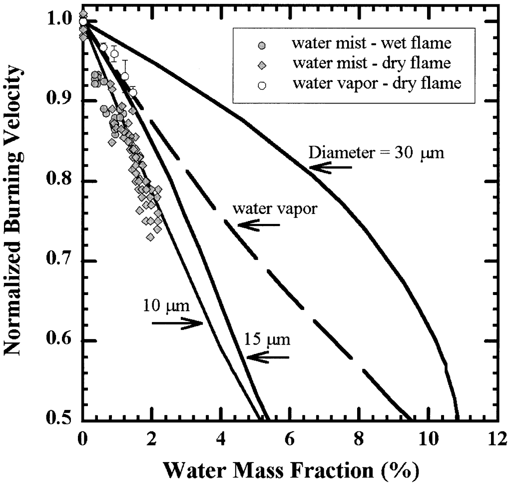

FIG. 5. Premixed methane/air burning velocity as a function of agent mass fraction, normalized by the uninhibited burning velocity: water data from Fig. 4 (symbols), multiphase flame modeling results for humidified flames inhibited with mists of indicated drop size (solid lines), and PREMIX modeling results for humidified flames inhibited with additional water vapor (dashed line).

times more effective at extinguishing flames than N_2 on a mass basis. A similar ratio of efficiencies was found in a modeling study of premixed methane/air flames [6]. These findings are consistent with our measurements, indicating that water mist can be at least as effective an inhibitor as CF_3Br on a mass basis. This is significant because water acts primarily as a physical suppression agent, while CF_3Br has a large chemical inhibition component.

Sheinson et al. [18] determined that the sensible enthalpy from 300 to 1600 K per mole O_2 for an agent at the extinction concentration for an *n*-heptane cup burner flame is comparable for most physical agents. To apply this formalism to the inhibition of these premixed flames, we have determined the sensible enthalpy per mole O_2 for the amount of agent required for a 20% burning velocity reduction. Results, given in column 6 of Table 1, show that the experimental value for water obtained for either the nominal 0.35-μm diameter mist drops or water vapor lie between those for N_2 and CF_4. Thus, water can contribute to flame inhibition in a manner comparable to that of inert gaseous agents. The significantly lower sensible enthalpy per mole O_2 determined for CF_3Br is an indication of a strong chemical inhibition component.

Flame modeling results for methane/air flames inhibited with mists of various drop size and flames inhibited with additional water vapor above the saturation limit at room temperature are shown in Fig. 5 along with the experimental data from Fig. 4. The modeled burning velocities are normalized with respect to the simulated, drop-free, water-vapor-saturated (100% relative humidity) methane/air burning velocity, which is found to be 33.5 cm/s. The prediction for the inhibition effect of additional water vapor is given by the dashed line, that agrees with the experimental observations. The mist experimental data, which lie on the small-drop-limit curve as seen in Fig. 5, are in excellent agreement with the multiphase model. It should be noted that there are no adjustable parameters in the model. The chemical reaction mechanism and the associated thermodynamic and transport properties are taken from GRI-MECH 3.0 [11], but with the nitrogen chemistry removed.

As seen in Fig. 5, the mist-inhibited burning velocity is predicted to decrease up to a water loading of about 2% (by mass), at which point the burning velocity is about 75% of the uninhibited burning velocity. According to the simulations, the mist-laden flames should continue to persist along the limit curve, with the burning velocity reduced to below 5 cm/s at a water loading of roughly 10%. The 30-μm model results in Fig. 5 predict that there is a turning-point behavior with increasing water loading. Both the computational and theoretical models predict such behavior for larger drops. Future experiments will focus on the effect of larger drops on the burning velocity behavior for these flames.

Summary

Measurements performed in this study indicate that water mist under the appropriate conditions can be as effective as CF_3Br on a mass basis at inhibiting premixed flames. Water mist was shown to be approximately 3.5 times more effective by mass than inert agents, N_2 and CF_4, and twice as effective as water vapor at reducing the methane/air burning velocity. These results are consistent with an evaluation of the thermodynamic properties, indicating that the thermal capacity of water mist can be used effectively in comparison with gaseous thermal agents, given suitable conditions. Water-mist-inhibited burning velocity measurements are also in excellent agreement with modeling predictions incorporating detailed combustion chemistry and multicomponent molecular transport, supporting the prediction of a small drop-size limit to the mist suppression effectiveness. Future research will investigate the effectiveness of larger drops and drops containing aqueous solutes capable of imparting a chemical component to the burning velocity reduction mechanism.

Acknowledgments

This work was supported by the Strategic Environmental Research and Development (SERDP) Next Generation

Fire Suppression Program, the Office of Naval Research through the Naval Research Laboratory, and NASA through the Center for the Commercial Applications of Combustion in Space (CCACS) at the Colorado School of Mines. The authors acknowledge the contributions of D. J. Dye for the development of the data acquisition programs and V. A. Shamamian for the use of the burner and atomizer.

REFERENCES

1. Babushok, V., and Tsang, W., *Combust. Flame* 123:488–506 (2000).
2. Seshadri, K., *Combust. Flame* 33:197–215 (1978).
3. Linteris, G. T., and Truett, L., *Combust. Flame* 105:15–27 (1996).
4. Noto, T., Babushok, V., Burgess Jr., D. R., Hamins, A., Tsang, W., and Miziolek, A., *Proc. Combust. Inst.* 26:1377–1383 (1996).
5. Reinelt, D., and Linteris, G. T., *Proc. Combust. Inst.* 26:1421–1428 (1996).
6. Noto, T., Babushok, V., Hamins, A., and Tsang, W., *Combust. Flame* 112:147–160 (1998).
7. Linteris, G. T., Burgess Jr., D. R., Babushok, V., Zachariah, M., Tsang, W., and Westmoreland, P., *Combust. Flame* 113:164–180 (1998).
8. Andrews, G. E., and Bradley, D., *Combust. Flame* 18:133–153 (1972).
9. Mitani, T., *Combust. Flame* 43:243–253 (1981).
10. Blouquin, R., and Joulin, G., *Proc. Combust. Inst.* 27:2829–2837 (1998).
11. Smith, G. P., Golden, D. M., Frenklach, M., Moriarty, N. W., Eiteneer, B., Mikhail Goldenberg, M., Bowman, C. T., Hanson, R. K., Song, S., Gardiner Jr., W. C., Lissianski, V. V., and Qin, Z., GRI-Mech 3.0, Gas Research Institute, Chicago, 2001, www.me.berkeley.edu/gri_mech/.
12. Yang, W., and Kee, R. J., *Combust. Flame* 130:322 (2002).
13. Lentati, A. M., and Chelliah, H. K., *Combust. Flame* 115:158–179 (1998).
14. Pitts, W. M., and Blevins, L. G., *An Investigation of Extinguishment by Thermal Agents Using Detailed Chemical Kinetic Modeling of Opposed Jet Diffusion Flames,* NISTIR 6588, National Institute of Standards and Technology, Gaithersburg, MD, 2000.
15. Kee, R. J., Grcar, J. F., Smooke, M. D., and Miller, J. A., *PREMIX: A Fortran Program for Modeling Laminar One-Dimensional Premixed Flames,* Sandia report SAND85-8240.
16. Parks, D. J., Alvares, N. J., and Beason, D. G., *Fire Safety J.* 2:237–242 (1979).
17. Chase Jr., M. W., Davies, C. A., Downey Jr., J. R., Frurip, D. J., McDonald, R. A., and Syverud, A. N., *J. Phys. Chem. Ref. Data* 14, (Suppl. 1):S48, S73, 1275, 1551 (1985).
18. Sheinson, R. S., Penner-Hahn, J. E., and Indritz, D., *Fire Safety J.* 15:437–450 (1989).
19. Hamins, A., Trees, D., Seshadri, K., and Chelliah, H. K., *Combust. Flame* 99:221–230 (1994).
20. Zegers, E. J. P., Williams, B. A., Fisher, E. M., Fleming, J. W., and Sheinson, R. S., *Combust. Flame* 121:471–487 (2000).

COMMENTS

Assaad Masri, University of Sydney, Australia. Are you planning to perform similar calculations for non-premixed flames where the strain rates and the residence times are different and changing? In addition, would you expect a similar conclusion regarding the droplet size effects?

Author's Reply. We are pursuing efforts to allow us to calculate water mist inhibited non-premixed counterflow flames. Water drops will experience longer characteristic residence times in counterflow flames than in premixed methane-air flames, except at very high strain rates (near extinction). Flames at higher strain rates are more easily extinguished although by presenting the water drops shorter residence times are available for the water drops. Thus, it is likely to expect a non-monotonic suppression behavior versus water loading in these flames as well.

•

Ariel Dvorjetski, Technion IIT, Israel. Would you suggest that the bifurcations found for premixed flames (D_{rp} size vs. S_{L}) would appear for diffusion counter-flow flames?

Author's Reply. The metric for suppression effectiveness in non-premixed (diffusion) counterflow flames is extinction. For methane-air and propane-air flames, we found a fairly monotonic decrease in the extinction strain rate with the addition of water drops below ~40 μm. For these flames, it may be reasonable to expect bifurcations in the extinction strain rate versus water loading curves for drops larger than 40 μm. Velocity slip in the strained counter flow velocity fields for these larger drops is an additional factor that will influence suppression behavior that is not present in the premixed configuration.

•

Takashi Tsuruda, National Research Institute of Fire and Disaster, Japan. In your figure, the diameter near 50 μm shows non-monotonic reduction of burning velocity. For real applications, do you think fine mist will work better than 50 μm drops?

Author's Reply. With a turning-point extinction behavior, drops larger than about 30 μm (for stoichiometric methane-air flames) affect burning velocity very differently than smaller drops. The abrupt falloff in the burning velocity predicted for large drops is experimentally found to be an extinction point. Thus, the larger drops are capable of extinguishing these flames at a much higher burning velocity (smaller burning velocity reduction) than are the smaller drops. Nevertheless, on a mass-loading basis, small drops are more effective in flame suppression, even though they do not lead to an abrupt turning-point extinction. From a practical point of view, distribution of the mist into a flame is an important consideration. Larger drops, which can have greater momentum, may be easier to disperse. In addition, to have comparable effectiveness to Halon 1301, it is important that the drops survive as liquid until they get into the flame. Initially, very small drops may lack the lifetime requirement for survival as well as the momentum to be successfully directed to the fire threat. A combination of small and large drops may be more effective depending on the fire environment. However, there are limitations to generating large quantities of very fine, submicron water drops for large-scale applications. Thus, we would expect the optimal drop size to be application-dependent, with a balance being struck between drop generation, delivery, and evaporation.